Computers & Graphics 97 (2021) 108–116

Contents lists available at ScienceDirect

Computers & Graphics

journal homepage: www.elsevier.com/locate/cag

Special Section on CAD & Graphics 2021

A novel computation method of hybrid capacity constrained centroidal power diagram

Liping Zheng, Yuyou Yao, Wenming Wu, Benzhu Xu, Gaofeng Zhang*

School of Computer Science and Information Engineering, Hefei University of Technology, Hefei 230601, China

ARTICLE INFO

Article history:
Received 28 January 2021
Revised 1 April 2021
Accepted 13 April 2021
Available online 23 April 2021

Keywords:
Power diagram
Hybrid capacity constraints
Centroidal
Density

ABSTRACT

Power diagrams, as a powerful extension of Voronoi diagrams, have been utilized in a wide range of applications in various fields. By imposing the capacity constraint and the centroid constraint to the ordinary power diagram, capacity-constrained power diagram and centroidal capacity-constrained power diagram can be obtained respectively, in which, all the capacity constraints are fixed values. However, some practical applications require a special kind of power diagrams, called hybrid capacity-constrained centroidal power diagrams, where not all capacity constraints are fixed values, and instead there are some capacities of sites constrained to intervals. To this end, we propose an iterative computation method for the power diagrams with hybrid capacity constraints. On the one hand, a weight evaluated method is introduced to update the weights of interval capacity-constrained sites, and Newton's method is applied to optimize the weights of fixed-value capacity-constrained sites. On the other hand, Lloyd's method is employed to move the sites to their respective mass centers. Experimental results prove that the proposed method can effectively compute the centroidal power diagram with hybrid capacity constraints.

1. Introduction

Voronoi diagrams have a wide range of applications and expansions in computational geometry. Power diagram, as an important extension of the Voronoi diagram, introduces the "weight" characteristic to sites, and redefines the distances. By imposing the capacity constraint to the ordinary power diagram, a Capacity-Constrained Power Diagram (CCPD) can be obtained. By introducing the centroidal constraint on a secondary basis, a Centroidal Capacity-Constrained Power Diagram (CCCPD) can be obtained. Compared to Voronoi diagrams, due to the "weight" characteristic, power diagrams have the characteristics of precise capacity constraint. Consequently, power diagrams have been widely used in many fields, such as blue noise sampling [1,2], mesh optimization [3], fluid simulation [4], computer animation [5], location-allocation problem [6], sector division [7], and grain structure representation of polycrystalline materials [8], etc.

Aurenhammer et al. first introduce the concepts, properties, computation methods, and applications of power diagrams [9,10]. Imai et al. [11] summarize the theory and application of planar power diagrams. Gavrilova et al. [12] construct the power diagram based on the planar Voronoi diagram. However, in these researches, the issue of capacity optimization is ignored.

Capacity is an important characteristic of power diagrams. Recently, a large number of researchers have a focus on the computation method to obtain a power diagram that meets the capacity constraints. Balzer et al. first propose a capacity-constrained power diagram generation algorithm for discrete space [13] and continuous space [14]. This algorithm combines the false position, one-by-one iteration, and Lloyd's method [15] to stably obtain the CCCPD. However, due to the point-by-point iteration strategy, this algorithm is a time-sonsuming approach in the view of computation process of CCCPD.

de Goes et al. [16] use Newton's method to optimize the weights, combined with the adaptive step-size gradient descent method proposed by Mullen et al. [17] to optimize the sites, and iteratively obtained CCCPD alternately. However, the weight optimization and site optimization interface with each other in the optimization process, and only have linear convergence. Bourne et al. [6] propose a generalized Lloyd's method to compute the Centroidal Power Diagram (CPD), and theoretically prove its linear convergence. Xin et al. [18] develop an L-BFGS method with super-linear convergence to compute the CCCPD with general distance, and apply it to blue noise sampling, displacement interpolation and polygon convex decomposition.

* Corresponding author.
E-mail address: g.zhang@hfut.edu.cn (G. Zhang).

https://doi.org/10.1016/j.cag.2021.04.007
0097-8493/

In recent years, Zheng et al. [19] propose a GPU-CPU hybrid algorithm to accelerate the computation of power diagrams, which uses the GPU-based JFA algorithm to render and construct power diagrams, and then couples with the L-BFGS method to obtain CCCPD. Compared to the state-of-art pure CPU power diagram computation algorithm, this method has a significant improvement in the computation efficiency of power diagrams.

In the existing power diagram researches, the preset capacity constraints of all sites are fixed values, and the capacity of each site is approximate with the respective preset value in CCCPD. However, due to the difficultly of setting precise capacity constrained values for all sites, there may be some sites with capacity constrained intervals in some practical applications, such as Location-Allocation Problem (LAP) [20], in which the hybrid capacity constraints are essential to be considered. To the best of our knowledge, this paper is the first research on the power diagrams with hybrid capacity constraints. To this end, we propose an iterative algorithm to compute the CPD with hybrid capacity constraints. The main contributions of this work are as follows:

1. Combining with the fixed-value capacity constraints and the interval capacity constraints, a novel power diagram is introduced, called Hybrid Capacity-Constrained Power Diagram (HCCPD). By imposing the centroidal constraint on a secondary basis, a Hybrid Capacity-Constrained Centroidal Power Diagram (HCCCPD) can be obtained.
2. A weight evaluated method is developed to optimize the weights of sites with interval capacity constraints, and a Variable Capacity-Constrained Power Diagram (VCCPD) can be obtained.
3. Coupling with Newton's method and Lloyd's method, our efficient computation method is proposed to compute the HCCCPD.

The remainder of this paper is organized as follows. Section 2 briefly reviews the preliminary of our method. Section 3 introduces the concepts of HCCCPD, and presents the iterative computation algorithm for HCCCPD. In Section 4, we illustrate our experimental results, and conclusions are given in Section 5.

2. Preliminary

In this section, we introduce the concepts of power diagrams, and some extensions of ordinary power diagrams.

2.1. Power diagram

The Voronoi diagram defines a spatial subdivision of a given domain Ω. That is, given a set of sites $\mathbf{X} = \{\mathbf{x}_i\}_{i=1}^n$, the Voronoi diagram is a partition of the domain Ω into n regions $\mathbf{V} = \{v_i\}_{i=1}^n$ based on the Euclidean distance. Voronoi cell v_i of the site $\mathbf{x}_i$ is defined as follow:

$$v_i = \left\{\mathbf{x} \mid ||\mathbf{x} - \mathbf{x}_i||^2 \le ||\mathbf{x} - \mathbf{x}_j||^2,\ for\ j = 1, ..., n\ and\ j \ne i\right\} \tag{1}$$

As an extension of Voronoi diagrams, power diagrams introduce a weight w_i to the site $\mathbf{x}_i$, and the power cell p_i of the site $\mathbf{x}_i$ is redefined as follow:

$$\begin{aligned} p_i = \Big\{\mathbf{x} \mid\ & ||\mathbf{x} - \mathbf{x}_i||^2 - w_i \le ||\mathbf{x} - \mathbf{x}_j||^2 - w_j, \\ & for\ j = 1, ..., n\ and\ j \ne i\Big\} \end{aligned} \tag{2}$$

where $d(\mathbf{x}, \mathbf{x}_i) = ||\mathbf{x} - \mathbf{x}_i||^2 - w_i$ is defined as the power distance. It should be mentioned that a power diagram degenerates to the Voronoi diagram when all the weights of sites are equal [9].

2.2. CCCPD

Due to the introduction of weight to each site, power diagrams have the characteristic of precise capacity constraints. By imposing the capacity constraint and the centroidal constraint to an ordinary power diagram, a CCCPD can be obtained.

Let $\mathbf{X} = \{\mathbf{x}_i\}_{i=1}^n$ denote n given points (also called sites), with associated capacity constraints $c_i > 0$. Assuming that $\rho(\mathbf{x})$ is a C^1-smooth density function on the domain Ω, the capacity (i.e., area or volume) of each power cell p_i can be computed:

$$m_i = |p_i| = \int_{p_i} \rho(\mathbf{x}) d\mathbf{x} \tag{3}$$

Therefore, the sum of the capacities of power cells is equal to the total capacity of the domain Ω, that is:

$$\sum_{i=1}^n m_i = \int_\Omega \rho(\mathbf{x}) d\mathbf{x} \tag{4}$$

The power diagram with capacity constraints can be obtained by adjusting the weight of each site until the capacity of site $\mathbf{x}_i$ is equal to the preset capacity c_i, that is, $m_i = c_i$. By imposing the centroidal constraint to the power diagram with capacity constraints, the CCCPD can be obtained, in which each site is located at its respective mass center, that is:

$$\mathbf{x}_i = \mathbf{x}_i^* = \frac{\int_{p_i} \mathbf{x}\rho(\mathbf{x}) d\mathbf{x}}{\int_{p_i} \rho(\mathbf{x}) d\mathbf{x}} \tag{5}$$

3. Hybrid capacity-constrained centroidal power diagram

In this section, we describe the concepts of HCCCPD in detail. Furthermore, an iterative algorithm is developed for computing HCCCPD.

3.1. Problem description

As mentioned above, by imposing the capacity constraint and the centroidal constraint to an ordinary power diagram, we can obtain a HCCPD and a HCCCPD, respectively. We first recall the notions used for a power diagram. Let $\Omega \subset E^d$ be a convex, closed, bounded and connected domain, $\rho(\mathbf{x})$ is a C^1-smooth density function on Ω. Let $\mathbf{X} = \{\mathbf{x}_i\}_{i=1}^n$ denote n given sites in Ω, $\mathbf{W} = \{w_i\}_{i=1}^n$ represent the associated weights. Then, the power diagram is a partition of the domain Ω into n disjoint convex polygons $\mathbf{P} = \{p_i\}_{i=1}^n$, where $p_i \cap p_j = \varnothing$ and $\sum_{i=1}^n p_i = \Omega$.

Without loss of generality, let $\mathbf{X}_f = \{\mathbf{x}_i\}_{i=1}^m$ be m $(0 \le m \le n)$ given sites with associated fixed capacity-constrained values $c_i \in \mathbf{C}_f = \{c_i\}_{i=1}^m$, $c_i > 0$. $\mathbf{X}_v = \{\mathbf{x}_i\}_{i=m+1}^n$ denote the remaining sites with associated capacity-constrained intervals $[c_i^{min}, c_i^{max}] \in \mathbf{C}_v = \{[c_i^{min}, c_i^{max}]\}_{i=m+1}^n$, where $c_i^{max} \ge c_i^{min} \ge 0$ and $\sum_{i=1}^m c_i + \sum_{i=m+1}^n c_i^{max} \ge \int_\Omega \rho(\mathbf{x}) d\mathbf{x} \ge \sum_{i=1}^m c_i + \sum_{i=m+1}^n c_i^{min}$. Consequently, the power diagram with hybrid capacity constraints satisfies that the capacity of each site with fixed-value capacity constraint is equal to its preset value, and the capacities of sites with interval capacity constraints are located in its preset intervals. In particular, the HCCCPD degenerates to a Variable Capacity-Constrained Centroidal Power Diagram (VCCCPD) when all sites are constrained to intervals. Then, similar to [10], the kernel problem of HCCCPD is to minimize the total cost:

$$\begin{aligned} & min\ Q(\mathbf{X}, \mathbf{W}) = \sum_{i=1}^n \int_{p_i} ||\mathbf{x} - \mathbf{x}_i||^2 \rho(\mathbf{x}) d\mathbf{x} \\ & s.t.\ m_i = |p_i| = c_i,\ i = 1, 2, ..., m \\ & \quad c_i^{max} \ge m_i = |p_i| \ge c_i^{min},\ i = m+1, m+2, ..., n \end{aligned} \tag{6}$$

In what follows, we introduce our iterative algorithm for progressively computing the HCCCPD. Similar to the algorithms proposed by de Goes et al. [16] and Xin et al. [18], the weight optimization and site optimization are separated in the optimization

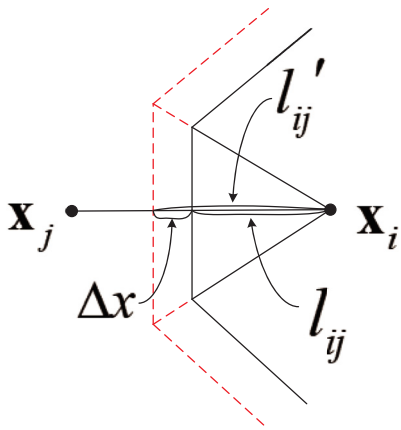

Fig. 1. Relationship of the weight of the site $\mathbf{x}_i$ and variation distance $\Delta\mathbf{x}_i$ of the equal power distance line.

process. Due to the existing of these sites with interval capacity constraints, the weight optimization of sites with fixed-value capacity constraints and interval capacity constraints are also separated. Specifically, there are three key operations in our iterative algorithm: (1) optimizing the suitable weights of sites with interval capacity constraints; (2) finding the optimal weights of sites with fixed-value capacity constraints by Newton's method; and (3) moving each site to the mass center of its corresponding power cell by Lloyd's method.

3.2. Weight optimization

3.2.1. Interval capacity constraint

For these sites associated with interval capacity constraints, the power diagram satisfies that the capacity of site $\mathbf{x}_i$ is located in the capacity-constrained interval $[c_i^{min}, c_i^{max}]$, that is, $c_i^{min} \le m_i = \int_{p_i} \rho(\mathbf{x})d\mathbf{x} \le c_i^{max},\ i = m+1, \ldots, n$. Based on the false-position method proposed by Balzer [14], we introduce a novel method, called weight evaluated method, to optimize the capacities of these sites with interval capacity constraints.

As shown in Fig. 1, let l_{ij} denote the distance between the site $\mathbf{x}_i$ and the equal power distance line, and $\Delta w_i = w_i' - w_i > 0$ indicate the variation of w_i. The variation distance Δx_i of the equal power distance line satisfies that: $l_{ij}' = l_{ij} + \Delta x_i$ after changing the weight w_i of the site $\mathbf{x}_i$. Zheng et al. [19] provide the calculation formula between Δx_i and Δw_i ($\Delta w_i > 0$) as follow:

$$\Delta x_i = \left\| \frac{w_i' - w_i}{2\|\mathbf{x}_j - \mathbf{x}_i\|^2}(\mathbf{x}_j - \mathbf{x}_i) \right\| = \frac{\Delta w_i}{2d_{ij}} \tag{7}$$

where d_{ij} is the Euclidean distance of $\mathbf{x}_i$ and $\mathbf{x}_j$.

It can be observed from Fig. 1 that the variation of the site capacity is closely related to the variation distance. However, the distances between neighboring sites and the site $\mathbf{x}_i$ are not the same, and even with the equal power distance line the variation distances are different. For the distant neighbor sites, the variation distances may be small, which are usually very large for the near neighbor sites. A large variation distance may cause the power cells of the near neighbor sites to be empty, which will affect the stability of the power diagram construction. Therefore, the variation of weight Δw_i can be calculated according to the distance d_i from the nearest neighbor site: $\Delta w_i = 2d_i \cdot \Delta x_i$, thereby eliminating the possibility that the power cell is empty during the optimization process. Consequently, for these sites with interval capacity constraints, updating the weight of the site whose capacity is less than its preset capacity-constrained interval using $w_i = w_i + 2d_i \cdot \Delta x_i$, and optimizing the weight of the site whose capacity is greater than its preset capacity-constrained interval using $w_i = w_i - 2d_i \cdot \Delta x_i$. The process is repeated until the capacity of each site is within the preset capacity-constrained interval. The procedure of the weight evaluated algorithm is given as follow:

Algorithm 1 Weight Evaluated Algorithm.

Input: sites $\mathbf{X}_v$, capacity constraints $\mathbf{C}_v$.
Output: VCCPD

```
repeat
    if there are sites with a capacity less than the left value
      of its preset constrained interval then
        Update its weight w_i = w_i + 2d_i · Δx_i
    end if
    if there are sites with a capacity greater than the right
      value of its preset constrained interval then
        Update its weight w_i = w_i − 2d_i · Δx_i
    end if
    Construct the power diagram
until capacities of all sites are within the preset capacity-
  constrained intervals
return VCCPD
```

3.2.2. Fixed-value capacity constraint

For these sites associated with the preset fixed capacity-constrained values, the power diagram strictly satisfies that the capacity of each site $\mathbf{x}_i$ meets to the preset value c_i, that is, $m_i = \int_{p_i} \rho(\mathbf{x})d\mathbf{x} = c_i,\ i = 1, 2, \ldots, m$. According to Eq. (6), the fixed-value capacity-constrained part in HCCCPD is to minimize the following total cost:

$$\begin{aligned} &Q(\mathbf{X}, \mathbf{R}) = \sum_{i=1}^{m} \int_{p_i} ||\mathbf{x} - \mathbf{x}_i||^2 \rho(\mathbf{x})d\mathbf{x} \\ &s.t.\ m_i = |p_i| = c_i,\ i = 1, 2, \ldots, m \end{aligned} \tag{8}$$

Aurenhammer et al. further prove that the optimal power diagram can be found by extremizing [10]:

$$F(\mathbf{X}, \mathbf{W}) = \sum_{i=1}^{m} \int_{p_i} ||\mathbf{x} - \mathbf{x}_i||^2 \rho(\mathbf{x})d\mathbf{x} - \sum_{i=1}^{m} w_i(m_i - c_i) \tag{9}$$

de Goes et al. [16] use Newton's method to find the optimal weight $\mathbf{W}$ to meet the preset capacity constraints while fixing $\mathbf{X}$. The gradient of $F(\mathbf{X}, \mathbf{W})$ in Eq. (9) w.r.t. w_i can be shown as:

$$\begin{aligned} &\nabla_{w_i} F(\mathbf{X}, \mathbf{W}) = c_i - m_i \\ &\nabla_{w_i} m_j = -\frac{\overline{\rho}_{ij}}{2} \cdot \frac{|e_{ij}^*|}{|e_{ij}|} \end{aligned} \tag{10}$$

where e_{ij} denotes the regular edge between two adjacent sites $\mathbf{x}_i$ and $\mathbf{x}_j$, e_{ij}^* represents the dual edge separating the power cell p_i and p_j, $\overline{\rho}_{ij}$ refers the average value of the field $\rho(\mathbf{x})$ over e_{ij}^*. The hessian matrix of $F(\mathbf{X}, \mathbf{W})$ in Eq. (9) can be computed based on Eq. (10). Consequently, Newton's method can be also applied to optimize the weights of these sites with fixed-value capacity constraints in HCCCPD. The procedure of Newton's method is given in Algorithm 2.

3.3. Site optimization

As mentioned above, by imposing the centroidal constraint to the HCCPD, a HCCCPD can be obtained, in which each site is located in the mass center of its corresponding power cell. Bourne et al. [6] propose Lloyd's method can be used to compute the CPD. Hence, Lloyd's method is also applied in our iterative algorithm to

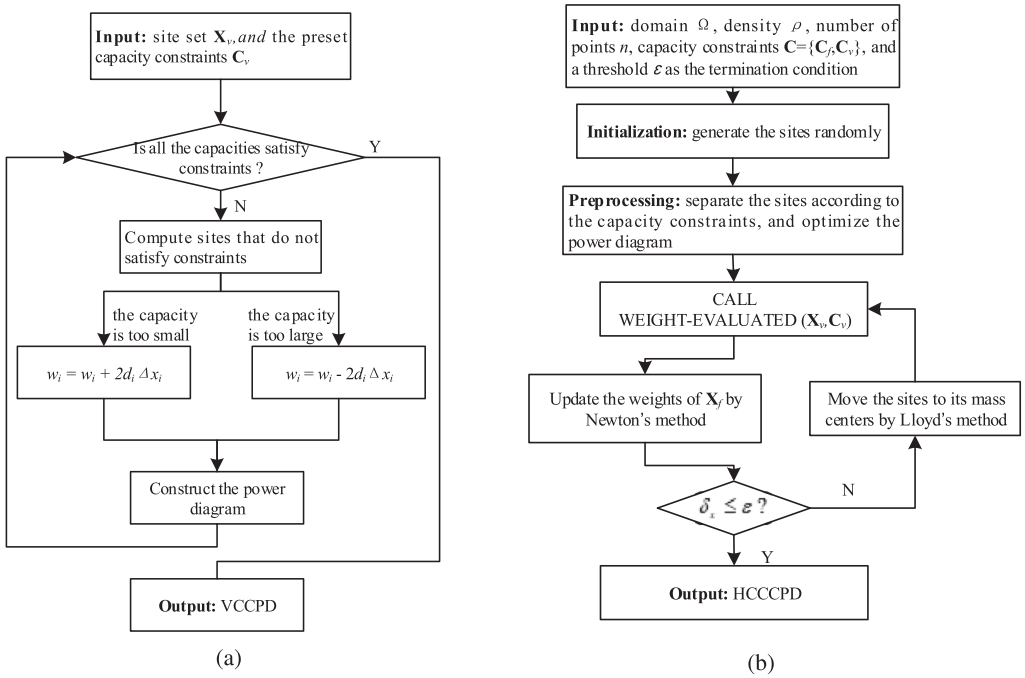

Fig. 2. The procedures of the proposed iterative algorithm for computing HCCCPD. (a) the weight evaluated algorithm; and (b) our proposed HCCCPD algorithm.

Algorithm 2 Newton's Algorithm.

Input: sites $\mathbf{X}_f$, capacity constraints $\mathbf{C}_f$.
Output: CCPD

```
repeat
    Compute the gradient and the hessian matrix of F(X, W)
      based on Eq. (10)
    Optimize the weights of sites X_f
    Construct the power diagram
until ||∇_W F(X, W)|| < 10^-12
return CCPD
```

move each site to its mass center. The centroid error δ_x can be computed in each iteration as follow:

$$\delta_x = \max\left\{\delta_{x_1}, \delta_{x_2}, ..., \delta_{x_n}\right\} \tag{11}$$

where $\delta_{x_i} = \|\mathbf{x}_i - \mathbf{x}_i^*\|^2$ denotes the squared distance between $\mathbf{x}_i$ and the mass center $\mathbf{x}_i^*$ of its corresponding power cell. Then, the final power diagram is obtained if the centroid error satisfies the termination condition. Otherwise, Lloyd's method is employed to optimize the site, and the next iteration is performed.

3.4. Iterative algorithm

Our iterative algorithm works as shown in Fig. 2. First, we start from a feasible site set $\mathbf{X}^{(0)}$ randomly generated in the domain Ω, and the weights of all sites are set to be equal. Assuming that $\mathbf{X}^{(k)}$, the sites in the k-th iteration, is a feasible site set as well, $\mathbf{W}^{(k)}$ is the weights in the k-th iteration. Next, we use the weight evaluated method to update the weights of sites with interval capacity constraints, and we compute the gradient and hessian matrix of $F(\mathbf{X}, \mathbf{W})$ based on Eq. (9), and employ Newton's method to update the weights of sites with fixed-value capacity constraints. Meanwhile, Lloyd's method is applied to update $\mathbf{X}^{(k)}$ to $\mathbf{X}^{(k+1)}$. Thus, the (k+1)-th iteration yields the next site set $\mathbf{X}^{(k+1)}$ and weights $\mathbf{W}^{(k+1)}$. This iterative process is repeated until the termination condition is satisfied. The pseudocode of our algorithm is given as follow:

Algorithm 3 HCCCPD Algorithm.

Input: domain Ω, density ρ, number of points n, capacity constraints $\mathbf{C} = \{\mathbf{C}_f, \mathbf{C}_v\}$, and a threshold ϵ as termination condition.
Output: HCCCPD

```
Initialization: set k = 0, and X = {X_f, X_v} to be n randomly
  generated sites
repeat
    Call Algorithm-1 to optimize the weights of sites X_v to
      meet the interval capacity constraints
    Call Algorithm-2 to optimize the weights of sites X_f to
      meet the fixed-value capacity constraints
    Compute the mass centers of power regions
    Move the sites to their respective mass centers using Llo-
      yd's method
    k = k + 1
until δ_x ≤ ε
return HCCCPD
```

3.5. Preprocessing

The calculation of the hessian matrix of $F(\mathbf{X}, \mathbf{W})$ is a crucial step in the weight optimization using Newton's method. In our algorithm, due to the combination of fixed-value capacity constraints and interval capacity constraints, the hessian matrix of $F(\mathbf{X}, \mathbf{W})$ may be irreversible, which may cause Newton's method to fail in the weight optimization process. To this end, we preprocess the site set $\mathbf{X}$ before the optimization to separate the sites with fixed value capacity constraints and those with interval capacity constraints. In this way, the irreversible situation of the obtained hessian matrix of $F(\mathbf{X}, \mathbf{W})$ can be effectively avoided.

In addition, the weight optimization of fixed capacity-constrained sites and interval capacity-constrained sites are separated in our iterative algorithm. Considering density field, there may be empty power cells during the weight optimization process when fixing the weights of interval capacity-constrained sites. To

Table 1
The preset capacity constraints of HCCCPD in our experiments.

HCCCPD	Capacity-constrained values	Capacity-constrained intervals
Fig. 3 (a)	0.020 (45)	[0.019, 0.021] (5)
Fig. 3 (b)	0.016 (45)	[0.055, 0.057] (5)
Fig. 3 (c)	0.018 (45)	[0.013, 0.015] (3), [0.0715, 0.0735] (2)
Fig. 3 (d)	0.010 (90)	[0.0095, 0.0105] (10)
Fig. 3 (e)	0.008 (90)	[0.0275, 0.0285] (10)
Fig. 3 (f)	0.009 (90)	[0.0055, 0.0065] (5), [0.0315, 0.0325] (5)

this end, the initialized power diagram should approximately satisfy the density distribution. That is, all sites are equipped with large interval capacity constraints, and the weight evaluated algorithm is applied to optimize the power diagram.

4. Experiment

In this section, we present the computational results to verify the efficiency of our iterative algorithm. We implement our algorithm in C++, and all the experiments are performed on a computer with 3.6 GHz Intel (R) Core (TM) i7-9700K CPU and 16 GB memory.

First of all, the basic test is performed in a squared domain with a side length of 1, centered at (0.5, 0.5). As mentioned in de Goes et al. [16], it usually takes 3–5 iterations to obtain the residual of capacity constraints within an accuracy of 10^{-12}. Therefore, the termination condition of Newton's method is set to 10^{-12}. Furthermore, based on the optimal results in [19], the variation Δx_i is set to 0.05, and the termination condition of Lloyd's method is set to 10^{-6}. The proportion of the number of interval capacity-constrained sites to the total number of sites is set to $\alpha = 10\%$. In addition, the default capacity-constrained interval is set to $\left[\overline{m} - \frac{\beta}{2} \cdot \overline{m}, \overline{m} + \frac{\beta}{2} \cdot \overline{m}\right]$, where $\overline{m}$ denotes the average capacity of each site, that is, $\overline{m} = \frac{\int_\Omega \rho(\mathbf{x}) d\mathbf{x}}{n}$, and the interval proportion β is set to 10%.

4.1. Constraint analysis

4.1.1. Result analysis

In this section, a comprehensive of computational experiments are conducted to verify the effectiveness of our proposed HCCCPD algorithm. The total number of sites is selected from $n \in \{50, 100\}$, where the number of interval capacity-constrained sites is $\alpha = 10\%$, and the interval proportion is $\beta = 10\%$. For simplication, the capacities of sites with fixed-value capacity constraints are equal, and the density $\rho(\mathbf{x})$ is selected as a uniform density, that is, $\rho(\mathbf{x}) = 1$.

Three different capacity-constrained intervals are considered in our experiments, as shown in Table 1. Fig. 3 illustrates the computational results of our proposed HCCCPD algorithm under different capacity constraints, where the blue and green regions are the corresponding power cells of sites with interval capacity constraints. From the results shown in Fig. 3, it can be observed that our proposed HCCCPD algorithm can effectively compute the centroidal power diagram with hybrid capacity constraints.

4.1.2. Parameter analysis

To illustrate the reliability of our proposed HCCCPD algorithm, we study the effect of the parameter α, which the proportion of the number of interval capacity-constrained sites to the total number of sites. In our experiments, the total number of sites are set to 100, and the proportion α is selected from $\alpha \in \{25\%, 50\%, 75\%, 100\%\}$. For simplification, the values of fixed-value capacity-constrained sites are equal, and the intervals of interval capacity-constrained sites are set to the default values. Fig. 4 shows

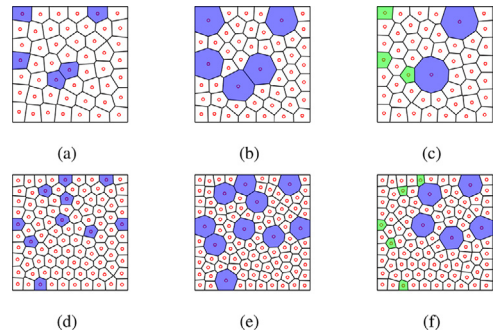

Fig. 3. The computational results of our proposed HCCCPD algorithm for 50 sites and 100 sites with uniform density. The first row: results for 50 sites. The second row: results for 100 sites. The first column: the power diagrams with the default capacity constraints. The second column: the power diagrams with large capacity-constrained intervals. The last column: the power diagrams with unequal capacity-constrained intervals.

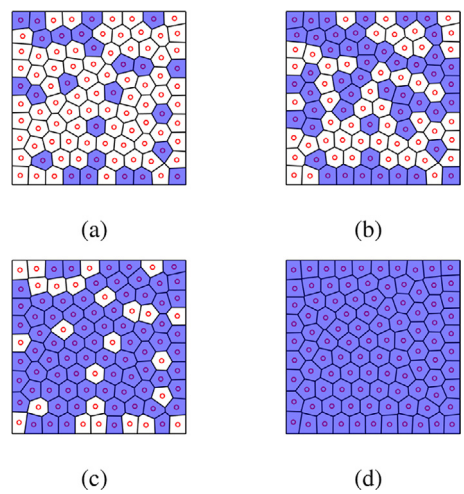

Fig. 4. The computational results under different values of the proportion α. (a) $\alpha = 25\%$; (b) $\alpha = 50\%$; (c) $\alpha = 75\%$; and (d) $\alpha = 100\%$.

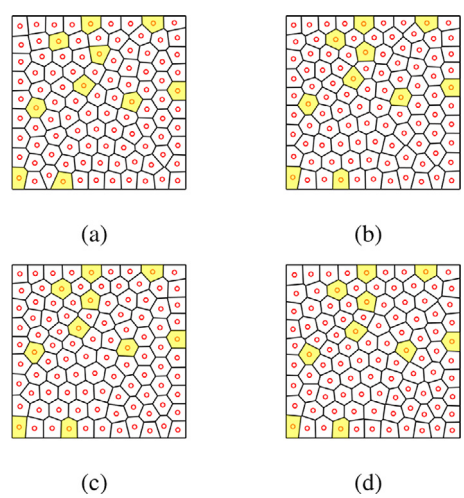

Fig. 5. The computational results under different values of the interval proportion β. (a) $\beta = 5\%$; (b) $\beta = 10\%$; (c) $\beta = 15\%$; and (d) $\beta = 20\%$.

the computational results with uniform density under different values of the proportion α, where the blue regions represent the corresponding power cells of these interval capacity-constrained sites.

Furthermore, we analysis the effect of the interval proportion β on the computational results. In this experiment, the propor-

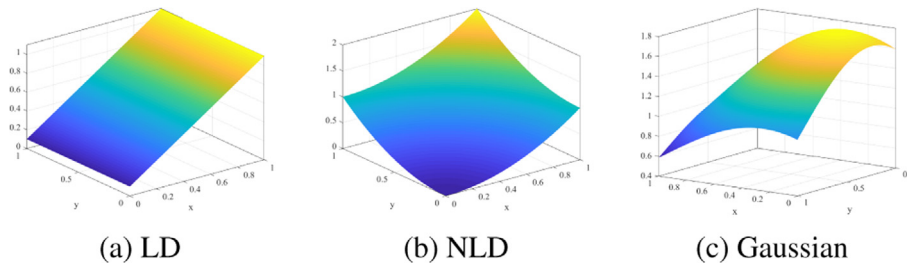

Fig. 6. Linear and non-linear densities in our experiments. (a) $\rho(x, y) = 0.1 + x$; (b) $\rho(x, y) = x^2 + y^2$; and (c) $\rho(x, y) = 1.8 \times e^{-[(x-0.25)^2+(y-0.25)^2]}$.

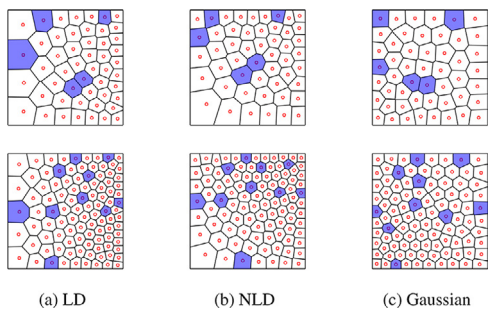

Fig. 7. The computational results of our proposed HCCCPD algorithm with three different densities. The first row: results for 50 sites. The second row: results for 100 sites. The first column: results with linear density. The second column: results with non-linear density. The last column: results with Gaussian density.

tion α is set to 90%, and the rest sites are set to fixed-value capacity constraints. The interval proportion β is selected from $\beta \in \{5\%, 10\%, 15\%, 20\%\}$. Fig. 5 illustrates the computational results with uniform density under different values of the interval proportion β, where the yellow regions denote the corresponding power cells of these fixed-value capacity-constrained sites.

From the results shown in Figs. 4 and 5, we can observe that our proposed HCCCPD algorithm is effective under different proportion α, and the computational results are different under various interval proportions. Particularly, when $\alpha = 100\%$, the centroidal power diagram with hybrid capacity constraints degenerates into a VCCCPD.

4.2. Density analysis

In order to verify the effectiveness of our proposed iterative algorithm in this paper, three types of densities are considered: Linear Density (LD), Non-Linear Density (NLD), and Gaussian Density (Gaussian). It is worth noting that Gaussian density is a special case of non-linear density, as illustrated in Fig. 6.

In the experiment, the number of total sites is set to $n \in \{50, 100\}$. The proportion of the number of interval capacity-constrained sites to the total number of sites is set to $\alpha = 10\%$, and the capacity-constrained intervals are set to the default intervals. Fig. 7 shows the computational results of our proposed HCCCPD algorithm with three different densities, where the blue regions denote the corresponding power cells of these sites with interval capacity constraints. It can be observed that our proposed HCCCPD algorithm can be well adapted to the general continuous density, and the results obtained are satisfactory.

4.3. Performance analysis

4.3.1. Computational time

The weight evaluated method and Newton's method are applied to update the weights in our proposed HCCCPD algorithm. We calculate the computational time of our proposed HCCCPD algorithm under various conditions. Four types of densities are experimented: uniform density (UD), linear density (LD), non-linear density (NLD), and Gaussian density (Gaussian). In our experiments, the interval proportion β is set to 10%, when analyzing the effect of the proportion α, and the proportion α is selected as 50% when testing the effect of the interval proportion β. The computational performance of our proposed HCCCPD algorithm is illustrated in Fig. 8.

Table 2
Comparison of computational time (in seconds) between two methods Xin et al. [18] and ours.

Method	Sites	Density		
		UD	LD	NLD
Xin et al. [18][1]	50	4.001	4.212	4.760
	200	14.107	22.412	28.319
Ours ($\alpha = 0\%$)[1]	50	2.204	3.039	2.871
	200	11.097	30.252	35.125
Ours ($\alpha = 100\%$)[2]	50	0.845	1.234	1.507
	200	7.209	15.124	17.998

[1] Power diagrams with fixed-value capacity constraints (CCCPD).
[2] Power diagrams with interval capacity constraints (VCCCPD).

According to the results shown in Fig. 8, we can observe that as the total number of sites raises, the computational time of our proposed HCCCPD algorithm also increases. On the one hand, when the number of interval capacity constrained sites increases, Newton's method is required to re-optimize the weights of fixed-value capacity constrained sites after the weight evaluated algorithm. Therefore, more computational time is required to compute the HCCCPD as the proportion increases. Besides, the interval proportion β also has a significant impact on the performance of the algorithm. When the capacity-constrained intervals are too small, the weight evaluated algorithm requires more iterations to optimize the weights of these sites with interval capacity constraints, and much more time consumption is required to compute the HCCCPD (e.g., $\beta \leq 2.5\%$).

4.3.2. Comparison

To further evaluate our proposed HCCCPD algorithm, we compare the experimental results obtained by our proposed algorithm with those obtained by the CCCPD algorithm proposed by Xin et al. [18]. To maintain consistency in these experiments, the squared region is selected as the default domain. In addition, the termination condition for Newton's method is set to 10^{-12}, and 10^{-6} is selected for Lloyd's method. Three types of densities are selected in our experiments: Uniform Density (UD), Linear Density (LD), and Non-Linear Density (NLD), as shown in Fig. 6. The computational performance is presented in Table 2, where the interval proportion β is set to 5%. Especially, when the proportion α is set to 100%, the HCCCPD degenerates to a VCCCPD, and the HCCCPD becomes a CCCPD when the proportion α is 0%. The computational results of two methods are illustrated in Fig. 9.

According to the computational results shown in Fig. 9, we can observe that our proposed HCCCPD algorithm is also effective for

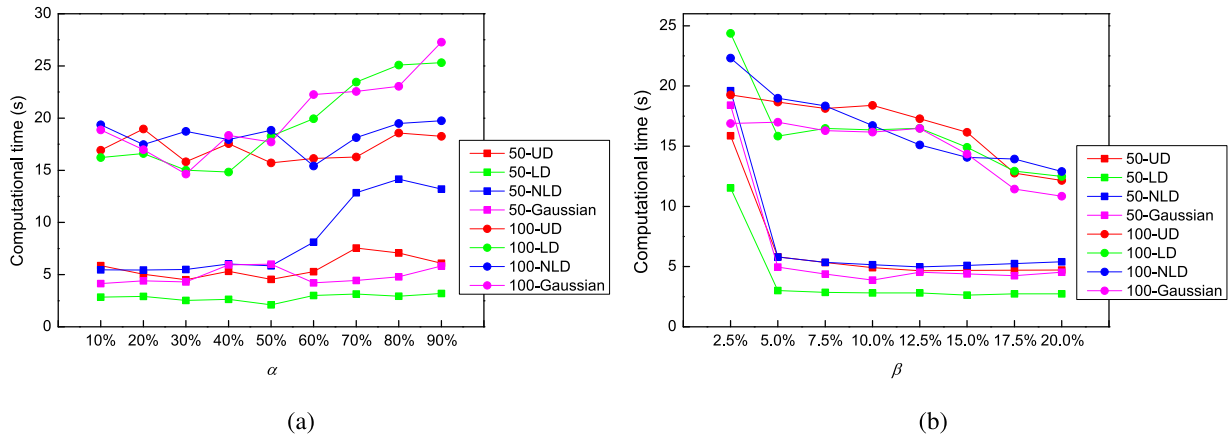

Fig. 8. The computational performance of our proposed HCCCPD algorithm under various conditions. (a) the relationship between the computational time and the proportion α, and (b) the relationship between the computational time and the interval proportion β.

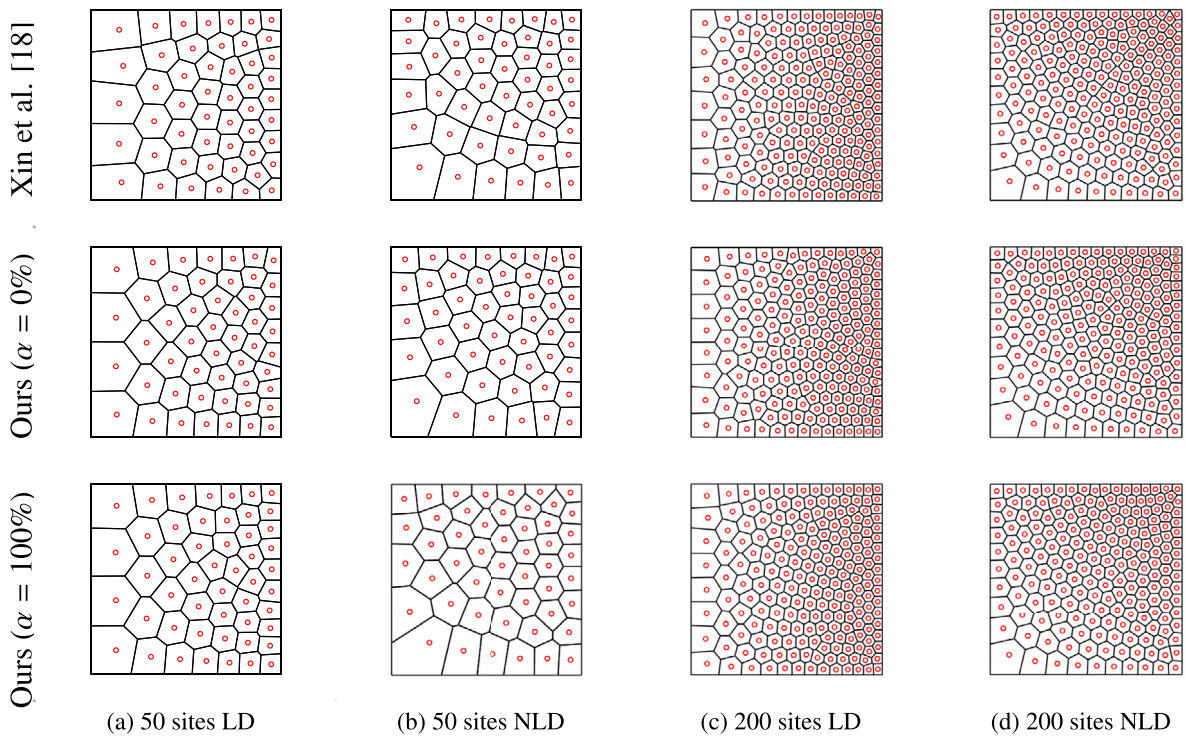

Fig. 9. The computational results obtained by our proposed HCCCPD algorithm and the algorithm proposed by Xin et al. [18]. The first row: results obtained by the algorithm proposed by Xin et al. [18]. The second row: results obtained by our proposed HCCCPD algorithm with $\alpha = 0\%$. The last row: results obtained by the HCCCPD algorithm with $\alpha = 100\%$ and $\beta = 5\%$. The first column: results for 50 sites with linear density. The second column: results for 50 sites with non-linear density. The third column: results for 200 sites with linear density. The last column: results for 200 sites with non-linear density.

some special power diagrams, such as CCCPD and VCCCPD. When the capacities of sites are constrained with intervals, that is, a VCCCPD, the results obtained by the two algorithms are similar, but the computational time of our proposed HCCCPD algorithm is less than the CCCPD algorithm in [18]. Since the CCCPD algorithm converges super-linearly, while Lloyd's method only converges linearly, our proposed HCCCPD algorithm is inferior to the CCCPD algorithm when computing the CCCPD. However, our proposed HCCCPD algorithm aims to compute the power diagrams with hybrid capacity constraints, and the purely CCCPD is just a special case.

4.4. More results

4.4.1. Complex domain

The domain is set to a squared region with a side length of 1 in the previous experiments. To demonstrate the computational results of our proposed HCCCPD algorithm in more complex domains, four different complex domains with uniform density are selected: triangle domain, non-convex domain, star domain, and circular domain. In our experiment, the total number of sites are 100, where the proportion α is set to 10%, and the interval proportion β is 10%. The computational results of our proposed HCCCPD algorithm under various domains are presented in Fig. 10, where the blue regions are the corresponding power cells of interval capacity constrained sites. It can be observed from Fig. 10 that our proposed HCCCPD algorithm is versatility, and reliable results can also be obtained for other complex domains.

4.4.2. More sites

We further study the effectiveness of our proposed HCCCPD algorithm in the case of more sites. The total number of sites are set from $n \in \{200, 500, 1000\}$, where half of the sites are set to

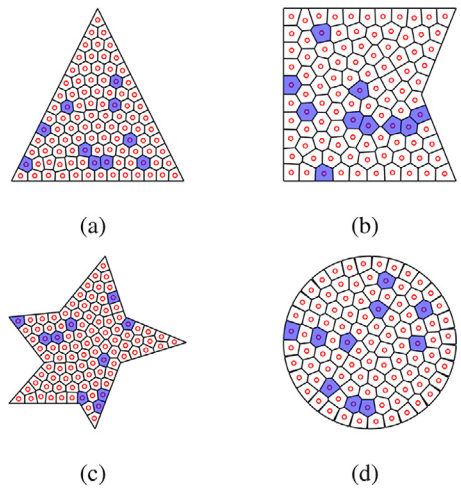

Fig. 10. The computational results of our proposed HCCCPD algorithm under various domains. (a) triangle domain; (b) non-convex domain; (c) star domain; and (d) circular domain.

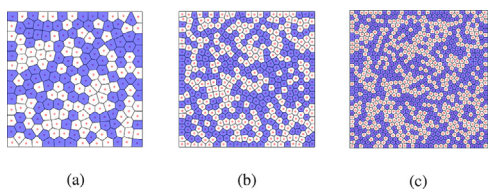

Fig. 11. The computational results of our propsed HCCCPD algorithm for different numbers of sites. (a) 200 sites; (b) 500 sites; and (c) 1000 sites.

interval capacity constraints, and the remaining sites are set to fixed-value capacity constraints. The domain is set to the default region with uniform density, and the interval proportion β is set to. Fig. 11 shows the computational results of our proposed HCCCPD algorithm for different numbers of sites, where the blue regions are the corresponding power cells of the interval capacity constrained sites. The results shown in Fig. 11 demonstrate that our proposed HCCCPD algorithm is effective to obtain the HCCCPD even with more sites.

5. Application

In this section we illustrate the feasibility of our proposed HCCCPD algorithm for the service region computation in the LAP [20]. The traditional LAP is to locate a set of facilities in a market region to meet the demands of customers. It is natural to use the CVT algorithm to determine the location and the service region of each facility [21,22], but the capacity of each facility is difficult to meet the predetermined value. Therefore, some weighted Voronoi diagrams are used to investigate the properties of allocation decisions, including multiplicatively weighted Voronoi diagram and power diagram [13,14], in which the capacities of facilities are definite values. However, it is difficult to determine the capacity of each facility in advance, and there may be some facilities whose capacity is set to an interval in practical applications. We adpot our proposed HCCCPD algorithm to compute the service regions of facilities in the LAP.

The distribution of urban population is crucial to the location of service centers. First of all, we collect census data online to obtain sample data of a certain city, which are mapped to a squared area with a side length of 50, centered at (35, 35). Then, the Newling mode is adopted to simulate the population density of this city. The density function is shown in Fig. 12(a).

$$\rho(x,y) = 27931 \times e^{-0.002\times[(x-29)^2+(y-45)^2]-0.001\times[(x-29)^2+(y-45)^2]^{\frac{1}{2}}} \tag{12}$$

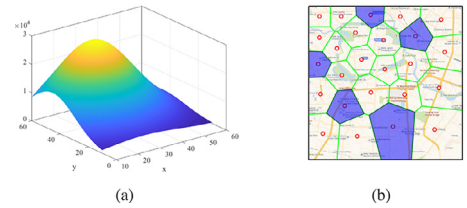

Fig. 12. The computational results for 25 service centers in a certain city. (a) density function; and (b) layout result.

Table 3
The detail data of the layout result in Fig. 12(b).

Capacity constraints	Centers location	Optimized capacity
[39.000, 41.000]	(13.063, 46.141)	39.007
50.000	(13.802, 31.389)	50.000
50.000	(13.464, 49.749)	50.000
50.000	(20.766, 37.523)	50.000
40.000	(14.609, 18.507)	40.000
[38.500, 41.500]	(21.704, 27.546)	40.421
50.000	(19.176, 46.244)	50.000
50.000	(13.487, 56.685)	50.000
50.000	(20.564, 56.647)	50.000
40.000	(25.779, 17.644)	40.000
[38.000, 42.000]	(30.150, 57.138)	41.060
50.000	(27.173, 42.654)	50.000
60.000	(30.220, 31.935)	60.000
40.000	(41.220, 31.255)	40.000
60.000	(25.207, 51.343)	60.000
[57.500, 62.500]	(37.417, 20.801)	58.657
40.000	(34.748, 39.464)	40.000
60.000	(34.365, 48.898)	60.000
50.000	(43.116, 41.257)	50.000
50.000	(39.815, 56.585)	50.000
[37.000, 43.000]	(44.731, 50.197)	40.855
50.000	(50.975, 19.848)	50.000
40.000	(54.256, 45.058)	40.000
50.000	(53.089, 55.609)	50.000
50.000	(52.384, 33.366)	50.000

∗ The capacities represent the population (in thousand) of service centers.

Assume that the total population in this city is 1.2 million, in the experiment, 25 service centers are to be located in this city, and two types of capacity constraints are considered: fixed-value capacity constraints and interval capacity constraints, as shown in the first column in Table 3. The final layout configuration of 25 service centers is presented in Fig. 12(b), where the red dots denote the location of service centers, the facets formed by segments represent the service regions of service centers, and the blue regions are the corresponding service regions of centers with interval capacity constraints. The detail data of service centers are illustrated in Table 3. The result in Fig. 12 and Table 3 prove that our proposed HCCCPD algorithm can effectively solve the LAP with hybrid capacity constraints.

6. Conclusions

In this paper, a novel power diagram is introduced, called the hybrid capacity-constrained centroidal power diagram. we propose a weight evaluated method to adjust the weights of sites to meet the variable capacity constraints. On this basis, an iterative algorithm is developed to compute the power diagrams with hybrid capacity constraints. On the one hand, the weight evaluated method is used to update the weights of interval capacity-constrained sites, and Newton's method is applied to optimize the weights of fixed-value capacity-constrained sites. On the other hand, Lloyd's method is employed to move the sites to the mass centers of its corresponding power cells. The experimental results prove that our

proposed HCCCPD algorithm can effectively compute the power diagrams with hybrid capacity constraints.

Limitation and future work. In our proposed HCCCPD algorithm, more time consumption is required when the interval proportion β is too small, as shown in Fig. 8(b). In our future work, we will extend our algorithm to improve its computational performance for the power diagrams with small interval capacity constraints.

Declaration of Competing Interest

The authors declare that they have no known competing financial interests or personal relationships that could have appeared to influence the work reported in this paper.

CRediT authorship contribution statement

Liping Zheng: Conceptualization, Methodology, Validation, Investigation, Writing - review & editing, Supervision, Funding acquisition. **Yuyou Yao:** Methodology, Software, Formal analysis, Investigation, Data curation, Writing - original draft, Visualization. **Wenming Wu:** Writing - original draft, Formal analysis. **Benzhu Xu:** Software, Resources, Supervision. **Gaofeng Zhang:** Conceptualization, Writing - review & editing, Project administration, Funding acquisition.

Acknowledgment

This study was partially supported by the National Natural Science Foundation of China (No. 61972128), and the Natural Science Foundation of Anhui Province, China (No. 1808085MF176).

References

[1] Zhang S, Guo J, Zhang H, Jia X, Yan DM, Yong J, et al. Capacity constrained blue-noise sampling on surfaces. Comput Graph 2016;55:44–54.
[2] Ahmed AG, Guo J, Yan DM, Franceschia JY, Zhang X, Deussen O. A simple push-pull algorithm for blue-noise sampling. IEEE TransVisComputGraph 2016;23(12):2496–508.
[3] Xiao Y, Chen Z, Cao J, Zhang YJ, Wang C. Optimal power diagrams via function approximation. Comput-Aided Des 2018;102:52–60.
[4] de Goes F, Wallez C, Huang J, Pavlov D, Desbrun M. Power particles: an incompressible fluid solver based on power diagrams. ACM Trans Graph 2015;34(4):1–11.
[5] Zheng L, Zhao J, Cheng Y, Chen H, Liu X, Wang W. Geometry-constrained crowd formation animation. Comput Graph 2014;38:268–76.
[6] Bourne DP, Roper SM. Centroidal power diagrams, lloyd's algorithm, and applications to optimal location problems. SIAM J Numer Anal 2015;53(6):2545–69.
[7] Li Z, Dai F, Jia H, Chang L. Research on the methods of multi-airport sector division based on a power diagram. In: ICCTP 2011: towards sustainable transportation systems; 2011. p. 3935–43.
[8] Alpers A, Brieden A, Gritzmann P, Lyckegaard A, Poulsen HF. Generalized balanced power diagrams for 3d representations of polycrystals. Philos Mag 2015;95(9):1016–28.
[9] Aurenhammer F. Power diagrams: properties, algorithms and applications. SIAM J Comput 1987;16(1):78–96.
[10] Aurenhammer F, Hoffmann F, Aronov B. Minkowski-type theorems and least--squares clustering. Algorithmica 1998;20(1):61–76.
[11] Imai H, Iri M, Murota K. Voronoi diagram in the Laguerre geometry and its applications. SIAM J Comput 1985;14(1):93–105.
[12] Gavrilova M, Rokne J. An efficient algorithm for construction of the power diagram from the Voronoi diagram in the plane. IntJComputMath 1996;61(1–2):49–61.
[13] Balzer M, Heck D. Capacity-constrained Voronoi diagrams in finite spaces. In: Proceedings of the 5th annual international symposium on Voronoi diagrams in science and engineering, 22 - 28 September, 2008, Kiev, Ukraine; 2008.
[14] Balzer M.. Capacity-constrained Voronoi diagrams in continuous spaces. IEEE; 2009. 2009 sixth international symposium on Voronoi diagrams, 79–88.
[15] Lloyd S. Least squares quantization in PCM. IEEE TransInfTheory 1982;28(2):129–37.
[16] de Goes F, Breeden K, Ostromoukhov V, Desbrun M. Blue noise through optimal transport. ACM Trans Graph 2012;31(6):1–11.
[17] Mullen P, Memari P, de Goes F, Desbrun M. Hot: Hodge-optimized triangulations. In: ACM SIGGRAPH 2011 papers; 2011. p. 1–12.
[18] Xin SQ, Lévy B, Chen Z, Chu L, Yu Y, Tu C, et al. Centroidal power diagrams with capacity constraints: computation, applications, and extension. ACM Trans Graph 2016;35(6):1–12.
[19] Zheng L, Gui Z, Cai R, Fei Y, Zhang G, Xu B. Gpu-based efficient computation of power diagram. Comput Graph 2019;80:29–36.
[20] Cooper L. Location-allocation problems. OperRes 1963;11(3):331–43.
[21] Du Q, Faber V, Gunzburger M. Centroidal voronoi tessellations: applications and algorithms. SIAM Rev 1999;41(4):637–76.
[22] Liu Y, Wang W, Lévy B, Sun F, Yan DM, Lu L, et al. On centroidal Voronoi tessellation-energy smoothness and fast computation. ACM Trans Graph 2009;28(4):1–17.